Improving the performance of a high power, lead–acid battery with paste additives

Troy C. Dayton [*], Dean B. Edwards

Department of Mechanical Engineering, University of Idaho, Moscow, ID, USA

Abstract

In this paper, we investigate the use of paste additives to improve the performance of a horizontal plate, lead–acid battery. The horizontal plate battery can deliver high power for electric and hybrid electric vehicle applications. We develop a series of designs having different paste additives to continuously improve the specific energy (W h/kg) performance of this battery. Computer models, previously developed and reported, are used to estimate the specific energy performance of these designs. The baseline, horizontal plate battery containing no additives has a specific energy of 30–35 W h/kg. The final design in our design progression uses both porous and conductive paste additives to provide an estimated specific energy of 60–70 W h/kg. © 2000 Elsevier Science S.A. All rights reserved.

Keywords: Lead–acid; Battery; Additives; Electric vehicle (EV); Power; Utilization

1. Introduction

The future of electric and hybrid electric vehicles are being widely discussed in the popular press, as well as by regulators and legislators. Invariably, much of the discussion centers on the most appropriate battery technology for these vehicles. Interestingly, studies done by the Jet Propulsion Laboratory [1,2] concluded that the most feasible electric vehicle (EV) is a limited range vehicle (i.e. ~ 100-mile range), and the most attractive battery for this vehicle is the lead–acid battery. In a study [3] conducted for the Department of Energy, the lead–acid battery was evaluated to have the highest technical merit and lowest developmental risk for use in electric vehicles when compared to other battery candidates. General Motor's electric vehicle, EV1, uses a sealed, lead–acid battery and demonstrates the validity of these studies.

Lead–acid batteries presently used in electric vehicles, however, are only modified versions of batteries designed for other applications. As such, they are proving to be inadequate for this demanding application, both with respect to life and performance. For lead–acid batteries to be successful in electric and hybrid electric vehicles, they must be designed specifically for those applications. In addition, these batteries need to be thermally managed and

their charging carefully controlled. The design of these batteries should also take advantage of this controlled operating environment.

One battery [4] designed specifically for electric vehicles uses multiple lug, horizontal plates and is shown in Fig. 1. The module shown in the figure has three cells with each cell consisting of a horizontal stack of double-lugged plates separated by glass-mat separators. The horizontal configuration allows the use of a multiple lugged conductor structure in order to achieve high specific power. This design feature effectively reduces grid resistance by shortening conductor lengths. The horizontal configuration also allows the use of mechanical containment where axial pressure is applied to the face of the positive electrode. Mechanical containment has been shown [5–8] to dramatically improve the life of lead–acid batteries. Cells were fabricated according to the design [4] shown in Fig. 1 and tested. The cells attained approximately 600 cycles (80% depth of discharge, DOD, at the 2-h rate) and had not failed before the tests were stopped. The projected specific energy for these cells operated at 110°F (43°C) was 35 W h/kg (2-h rate). The specific power was measured to be approximately 200 W/kg (80% DOD).

In this paper, we will modify the design previously presented [4] so as to improve its use in an electric vehicle or a range extended, hybrid electric vehicle (REHEV). A REHEV operates mostly as an electric vehicle but uses a
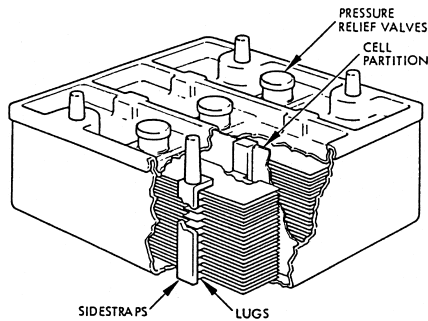
---

[*] Corresponding author.

Fig. 1. Sealed, lead–acid battery module.

small heat engine and alternator to charge its batteries during long trips. The battery requirements for these two vehicles are similar because both vehicles have significant electric vehicle range and need a high specific energy. The REHEV battery will not be as large as the electric vehicle battery and so will need to deliver more power per weight than the equivalent electric vehicle battery. However, the battery requirements for these two vehicles are similar so that a generic battery can be designed for both vehicle types.

In a previous paper [9], the design shown in Fig. 1 was modified for use in a parallel hybrid electric vehicle where the battery acts to load level the heat engine. The modified design was projected to achieve a specific energy of 22 W h/kg at a specific power of 550 W/kg. At a reduced power of 31.8 W/kg, the battery was projected to have a specific energy of 31.6 W h/kg and an energy density of 92.3 W h/l. Additives, in the form of glass microspheres, were added to the paste to achieve this performance. However, in this design the specific energy was reduced in order to increase the specific power. We realized that we could have improved the specific energy much more if we had not needed to meet the high specific power requirements and this knowledge encouraged us to write this paper.

In this paper, we will investigate the use of paste additives in battery designs and determine how they can improve the performance of sealed, lead–acid batteries in REHEV and electric vehicles. We will use the design reported in Ref. [4] as the baseline design. We will design batteries having different additives including glass microspheres, porous glass microspheres, and metal-coated, porous glass microspheres. The designs will show how the performance can be progressively improved with the use of additives. We will employ models previously developed [10–14] to estimate this performance improvement. We will show how, with a realistic development program, the lead–acid battery can meet the performance requirements for these vehicles.

In Section 2, we will discuss the models used to estimate the performance of the designs developed in this paper. We will document the models by comparing their results with the test results of the baseline design. In subsequent sections, we will design batteries having different additives and estimate their performance with our models. After we have evaluated the design, we will discuss the results. Section 9 will summarize and give our conclusions.

2. Models

In an attempt to better understand lead–acid batteries and the physical processes that limit capacity, computer models were developed that simulate the conductivity of the positive active material and the diffusion of sulfate ions. Researchers [15,16] have found that after a certain amount of the active material has reacted the remaining material becomes isolated and cannot react. The amount of active material that can be discharged before the remaining material becomes isolated is termed the critical volume fraction. Values for the critical volume fraction have been estimated to be approximately 60–70% for homogeneous paste. A model has been developed, called the conductivity model, that estimates the critical volume fraction of paste containing non-conducting or conducting additives [10].

In order to model the conductivity of the active material, the material is assumed to be made of spherical particles and modeled as nodes on a two-dimensional grid. Each node is connected to the surrounding eight nodes by a conductive pathway. The grid contains over one million nodes, 1024×1024 nodes. The model randomly chooses a node and attempts to find a conductive pathway to the edge of the grid. If a pathway can be found, the starting node is considered discharged and marked as non-conductive. If a pathway is not found, the starting node is marked as isolated. After all nodes have been selected and pathways have been tried, the model reports the number of nodes that were either discharged or isolated. The critical volume fraction is calculated as the ratio of discharged nodes to the initial number of available nodes.

The model can take into account any non-conductive additives by initially marking those nodes as discharged. For conductive additives the model marks those nodes as always conductive. The amounts of additives are given as volume percentages and the size of the individual additive is given relative to the base node size. For example, a non-conductive glass microsphere, approximately 20–50 μm in diameter, is represented as a particle of 10×10 nodes. Using this model, Fig. 2 [14] was created to show the effect on the critical volume fraction of adding conductive and non-conductive additives.

The second model, called the diffusion model, uses finite difference equations and Fick's law to estimate the acid concentration in both the negative and positive material as well as between them as a function of time. The Nernst equation is then used to determine the battery potential. The model combines diffusion and conductivity parameters, including the critical volume fraction from the
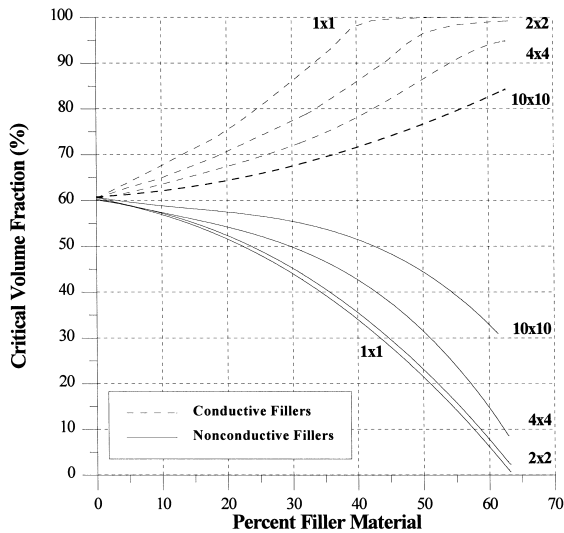
Fig. 2. Critical volume fraction with material additives.

conductivity model, to estimate lead–acid battery performance over a wide range of discharge rates. The model produces voltage vs. time curves, percent material reaction curves, and acid concentration plots. The model is helpful in understanding the behavior of lead–acid batteries and can be used to develop new cell designs. Once the plate and cell parameters are established, the model can predict the cell's performance and allows for iterations to determine optimum parameter values.

3. Electric vehicle requirements

In order to develop a good battery design, we must first understand how it will be used. We will establish the power requirements for the battery from a previously reported electric vehicle design [17] for a lead–acid battery. This electric vehicle can be characterized by a few critical parameters which define the road load. The road load equation determines the battery power required to maintain the vehicle at a given speed and is given as:

$$P_B(V) = \frac{1}{\eta_G \eta_M} \left(\frac{1}{2} \rho_A C_D A V^3 + \mu M g V \right)$$

where $\rho_A = 1.2929$ kg/m^3, $g = 9.8$ m/s^2, V is the velocity in m/s and the other parameters are given in Table 1.

Table 1
Electric vehicle parameters

Parameter	Value
Motor to wheel gear efficiency (η_G)	0.95
Motor efficiency (η_M)	0.90
Drag coefficient (C_D)	0.32
Frontal area (A)	1.88 m^2
Rolling resistance μ	0.009
Total vehicle weight (M)	1606 kg
Battery weight	600 kg

Table 2
Battery design parameters

Parameters	Values
Positive plate	
Grid thickness	0.071 in. (0.18 cm)
Grid volume	3.2 cm^3
Grid weight	35 g
Plate thickness	0.076 in. (0.19 cm)
Paste weight	69 g
Critical volume fraction	60%
Number positive plates	14
Negative Plate	
Grid thickness	0.060 in. (0.15 cm)
Grid volume	2.7 cm^3
Grid weight	30 g
Plate thickness	0.067 in. (0.17 cm)
Paste weight	57.3 g
Critical volume fraction	65%
Number negative plates	15
Effective distance between plates	0.0572 in. (0.145 cm)
Electrolyte volume	765 cm^3
Electrolyte specific gravity	1.3 g/cm^3
Electrolyte initial concentration	5.1 mols/l
Misc. weights (terminals, straps, etc.)	246 g
Case weight	246 g
Total weight	4.253 kg

Using the vehicle parameters and the road load equation, the power required of the batteries at a speed of 55 miles/h (24.6 m/s) is 10.8 kW. For the battery pack weight of 600 kg, the specific power is 18 W/kg. At a speed of 70 miles/h (31.3 m/s), the battery power required is 19 kW and the specific power is 31.7 W/kg. With these power requirements, the effectiveness of a battery design powering an electric vehicle can be established.

This vehicle design has been considerably improved upon by the General Motors Impact electric vehicle introduced in 1992. With its improved aerodynamics and low rolling resistance tires it has an approximate road load of 5.5 kW at 55 miles/h and 9.5 kW at 70 miles/h. With its 500-kg battery pack, the Impact requires a specific power of 11 and 19 W/kg for speeds of 55 and 70 miles/h, respectively.

4. Baseline battery

The baseline battery for this research was developed at the Jet Propulsion Laboratory (JPL) to be used in an electric vehicle application. The design consists of horizon-

Table 3
Baseline battery design test results

Test parameter	Average results
Energy discharged	150 W h
Specific energy	35.4 W h/kg

Table 4
Model results of baseline battery design

Discharge rate (A)	Time (s)	Discharge (Ah)	Utilization (%)
2.70	7198	5.40	34.91
5.00	3633	5.05	32.63

tally oriented, dual lugged plates in a sealed configuration [4]. Table 2 shows the design parameters for this battery. This battery was built and tested by personnel at JPL.

Using these parameters, the baseline battery design was modeled and the cell discharge was simulated. Table 3 gives the performance of this battery at a discharge rate of 18 W/kg, approximately the 2-h rate. The model predicts a discharge energy of 150 W h and a specific energy of 35.4 W h/kg at the 2-h rate. Table 4 gives the utilization of the positive active material predicted by the model when the baseline cell is discharged at the 18 and 32 W/kg rates. The specific power of 32 W/kg corresponds to a discharge rate close to the 1-h rate. A discharge energy of 142 W h and a specific energy of 33.5 W h/kg were predicted by the model at the 1-h rate (see Table 5).

Fig. 3 shows the profiles of the reacted material every 2000 s for the 2-h discharge rate. The active material is reacted up to the critical volume fraction at the edge of both the negative and positive plates. A portion of the interior active material also reacts. The overall utilization is given in Table 4 as approximately 35%. Comparison of the 2-h rate discharge with those reported by JPL suggest that the model can accurately predict the performance of this cell design. The rest of this paper assumes that the accuracy of the model continues through several iterative cell designs. The performance predicted by the model will be the basis for determining the effectiveness of cell designs with additives.

Fig. 4 shows a plot of specific energy (W h/kg) versus specific power (W/kg). This figure shows the 1- and 2-h discharge rates as reference lines of specific power. The 2-h discharge rate (18 W/kg) for this battery design corresponds with the road load for a typical electric vehicle traveling at 55 miles/h. Likewise, the 1-h discharge rate (32 W/kg) represents an electric vehicle speed of 70 miles/h. Therefore, the baseline battery design would be able to power an electric vehicle 2 h at a speed of 55 miles/h, for a maximum range of 110 miles. Alternatively, the electric vehicle could be powered for 1 h at a speed of 70 miles/h, for a maximum range of 70 miles.

The model results for this design, and the results for all subsequent designs, will be used to predict cell performance at the specific powers of 18 and 32 W/kg. Using these specific powers, we can compare the results of the computer simulations for different designs and establish the effectiveness of the designs for EVs and REHEVs. In the following sections, we investigate using different paste additives in the horizontal battery design and compare these designs using specific energy versus specific power plots.

5. Design with glass microspheres

As shown in Table 4, only 35% of the active material in the positive plate of the baseline battery is reacting. It would be weight effective to remove the portions that do not react. Non-conducive glass microspheres can be added to the positive material as a filler to replace material that is not reacting. These microspheres are approximately 10 times larger than the lead oxide particles and have a density approximately 20 times less. If 30% by volume of large additives (10×10) are added to the positive active material, the critical volume fraction is reduced from 60% to 55%, as shown in Fig. 2. It is assumed that the additives will displace lead oxide material and not occupy any of the pore volume. Therefore, the 30% by volume number is with respect to the volume of the lead oxide particles. This

Table 5
Results of model with additive types at specific powers of 18 and 32 W/kg

| Additive type	Specific power (W/kg)	Energy (W h)	Increase (%)	Specific energy (W h/kg)	Increase (%)
None	18	151.0	–	35.5	–
	32	142.0	–	33.5	–
30% Microspheres	18	155.0	2.6	47.0	32.4
	32	145.0	2.1	44.0	31.3
23% Porous, microspheres	18	182.5	20.9	50.0	40.8
	32	171.5	20.8	47.0	40.3
30% Conductive, porous, microspheres	18	195.0	29.1	56.0	57.8
	32	184.0	29.6	53.0	58.2
20% Small, conductive + 10% porous, microspheres	18	206.0	36.4	63.0	77.5
	32	196.0	38.0	60.0	79.1
30% Small, conductive, porous, microspheres	18	216.5	43.4	68.5	93.0
	32	207.0	45.8	65.5	95.5
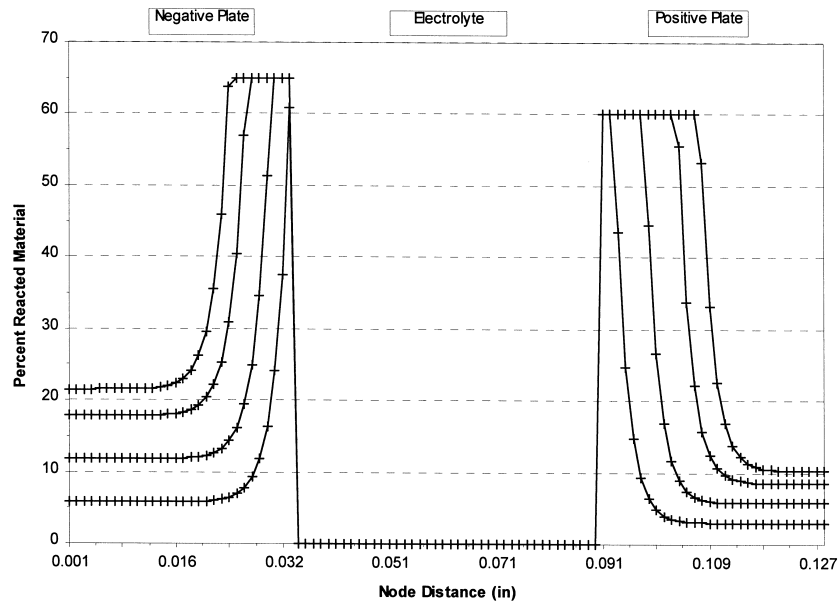
Fig. 3. Profiles of reacted material every 2000 s of baseline battery at 2-h discharge rate.

assumption holds for all the battery designs presented in this paper. With the addition of the additives, the positive active material (PAM) weight is reduced 30% from 69 to 48.3 g. To keep the battery design consistent, the negative active material (NAM) weight, grid volumes and weights, misc. weights and case weights are also reduced by 30%. The electrolyte volume and weight is not reduced since the PAM and NAM volumes on the plates did not change. The addition of the glass microspheres increases the total cell weight by only 1%. Due to the reduction in PAM weight for each individual plate, the corresponding cell needs an additional six plate pairs.

For this design, the energy discharged at specific powers of 18 and 32 W/kg is 155 and 145 W h, respectively. This increase in discharged energy is due to the increase in utilization of the positive active material, as listed in Table 5. Fig. 5 shows the profiles of reacted material every 2000 s for the specific power of 18 W/kg. Even though the critical volume fraction has been reduced, the overall utilization has increased since more interior material can react. Fig. 7 shows that at a specific power of 18 and 32 W/kg the specific energy increases to 47 and 44 W h/kg, respectively. Table 5 summarizes the model results and shows that by adding non-conducting additives the specific
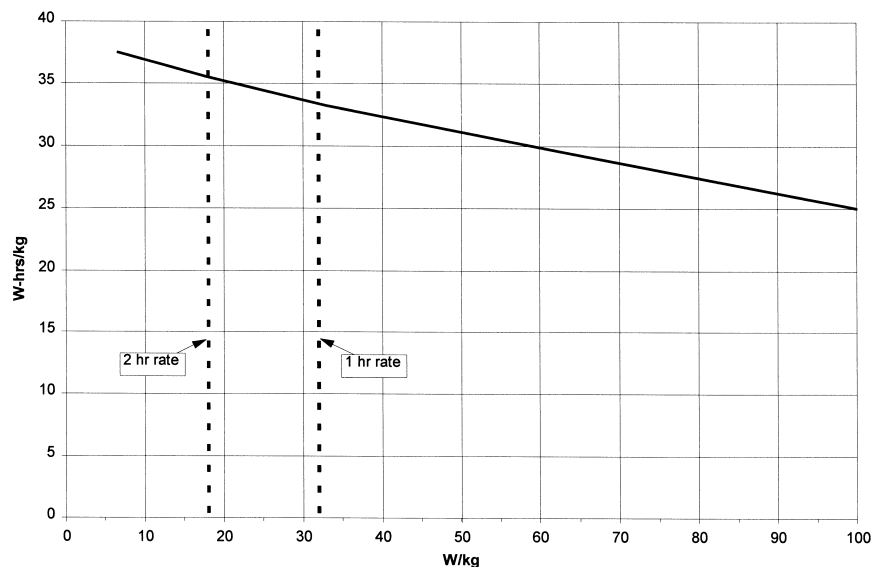

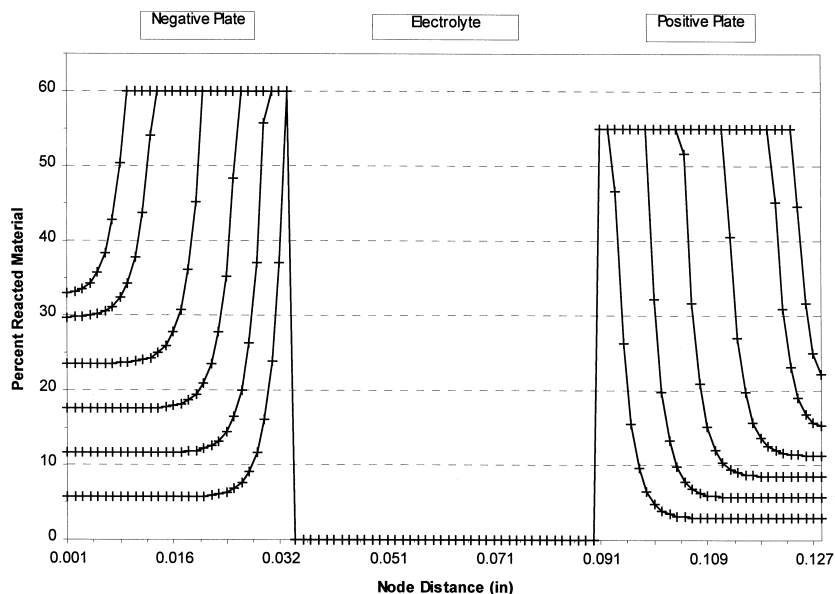Fig. 4. W h/kg versus W/kg for baseline cell design.

Fig. 5. Profiles of reacted material every 2000 s of design with glass microspheres at 18 W/kg.

energy increased 31–32% to a specific energy of approximately 45 W h/kg. This increase is due to the 22.3% reduction in plate weight and a 16% increase in utilization.

6. Design with porous, glass microspheres

In the next iteration on this battery design, we used porous glass microsphere additives in the positive material. The glass microspheres are 90% hollow, so by simply making holes in the microspheres, a porosity of 90% can be achieved. The reason for considering a porous additive is that the porosity of the active material can be increased

since the additive can be used as electrolyte storage within the active material. If 23% by volume of porous, glass microspheres are added to the positive and negative active material, the porosity of the positive active material increases from 45% to 65% and the porosity of the negative active material increases from 50% to 70%. The critical volume fraction is 57% and 62% for the positive and negative active material, respectively. The electrolyte stored in the porous additives in the active material does increase the cell weight. Energy discharged at specific powers of 18 and 32 W/kg increase to 182.5 and 171.5 W h and the specific energies increase to 50 and 47 W h/kg, as shown in Fig. 7. Table 5 indicates that this represents a 40%
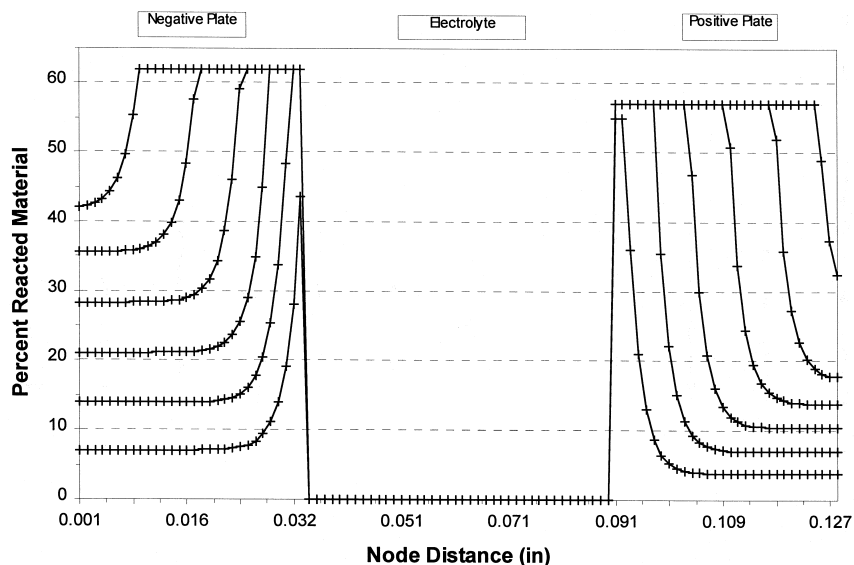

Fig. 6. Profiles of reacted material every 2000 s of design with 23% porous microspheres at 18 W/kg.
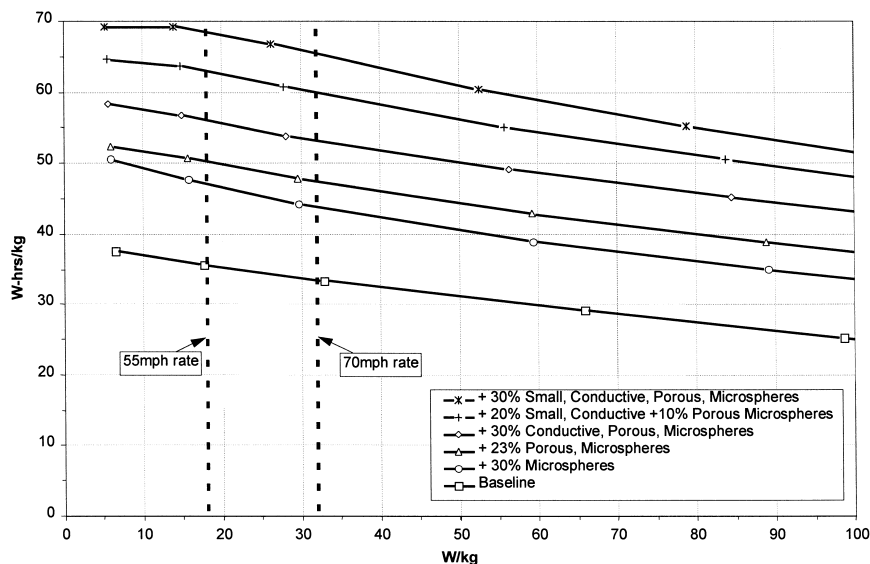
Fig. 7. Specific energy (W h/kg) versus specific power (W/kg) for all cell models.

increase in specific energy over the baseline battery design.

Fig. 6 gives the profiles of the reacted material every 2000 s for the specific power of 18 W/kg. The figure shows that for this cell design the critical volume fraction in the positive active material of 57% has nearly been reached at this discharge rate. Therefore, this design has reached the point where conductivity is limiting the performance. If more glass microspheres were added to the active material there would be no further increase in performance. In order to further increase the battery performance, conductive additives will be needed to raise the critical volume fraction of the active material.

7. Design with conductive, porous, glass microspheres

In the next iterative design step, we used conductive, porous glass microspheres to increase the conductivity and the critical volume fraction of the active material. Assuming the porous, glass microspheres can be coated with a conductive coating, the conductivity model predicts that the critical volume fraction increases by 12% with a 30% addition of large (10×10) conductive additives, as shown in Fig. 2. The critical volume fraction for the PAM and NAM increases to 67% and 72%, respectively. With this change the model predicts an energy discharge of 195 and 184 W h and a specific energy of 56 and 53 W h/kg for specific powers of 18 and 32 W/kg, respectively.

Fig. 7 shows how the specific energy of this design compares with the other designs. Table 5 gives values for the energy discharged and specific energy of this design. The performance of the design is limited by the critical volume fraction of the active material. According to Fig. 2,

a higher increase in the critical volume fraction can be accomplished by using smaller, conductive additives.

8. Designs with smaller, conductive, porous, glass microspheres

As shown in Fig. 2, when 20% by volume of small additives (1×1) are included in the active material the critical volume fraction increases to 75%. If 10% by volume of large microspheres ($> 10 \times 10$) are also added the critical volume fraction does not decrease significantly. If both the conductive additive and the large microspheres are considered porous, the net results are added paste porosity (27%) and increased conductivity (15%). To provide the needed electrolyte, the active material thickness in both the negative and positive plates are reduced by 7%. This distance between grids remains the same, thus the volume between plates has increased so more electrolyte may be added. For the specific powers of 18 and 32 W/kg, the resulting energy discharges are 206 and 196 W h with specific energies of 63 and 60 W h/kg. This cell design is limited by the conductivity of the active material.

When 30% by volume of small additives (1×1) are included in the active material the critical volume fraction increases to 85%, as shown in Fig. 2. If these small additives are again considered porous we then have added porosity (27%) and increased conductivity (25%). To provide the needed electrolyte, the active material thickness in both the negative and positive plates are reduced an additional 8%. For the specific powers of 18 and 32 W/kg, the resulting energy discharges are 216.5 and 207 W h with specific energies of 68.5 and 65.5 W h/kg. This cell design is also limited by the conductivity of the active material but since we are currently reacting 85% of the

positive active material, it is unlikely we can realistically increase the critical volume fraction any higher.

Fig. 7 shows how the specific energy has been increased with the use of small conductive additives in these two models. At specific powers of 18 and 32 W/kg the specific energies are nearly double the baseline battery design and the discharge times have increased by a factor of 2.5.

9. Conclusions

The baseline, horizontal plate battery containing no additives has a specific energy of 30–35 W h/kg. This battery is designed to have a high specific power to meet the demands of electric and hybrid electric vehicles. This paper has demonstrated, through a series of battery designs having different paste additives, that the specific energy performance can be significantly improved. With the addition of 30% by volume of conductive, porous, glass microspheres in the negative and positive active materials the specific energy can be increased by 58% to an estimated 50–60 W h/kg. If smaller additive sizes are considered, the specific energy can be increased 95% to an estimated 60–70 W h/kg.

By increasing the specific energy of the baseline battery design the feasibility of using lead–acid batteries in electric and hybrid electric vehicles increases. When the discharge times are examined, the final cell design discharged at the original 1- and 2-h rates would have discharge times nearly double the baseline. This means that for the same battery size and weight, the new cell design would almost double the range of present electric or hybrid electric vehicles.

We realize that these projections are based on theoretical models and that much work needs to be performed in order to validate these designs. However, we believe the strategy provided in this paper could lead to a substantially improved high power, lead–acid battery.

References

[1] K. Hardy et al., Advanced Vehicle System Assessment, JPL D-230, Jet Propulsion Laboratory, Pasadena, CA, 1983.

[2] G.L. Henriksen, D.L. Douglas, C.J. Warde, National Program Plan for Electric Vehicle Battery Research and Development, DOE/ID-10219, 1989.

[3] E.Z. Ratner, P.C. Symons, W. Walsh, C.J. Warde, Assessment of Battery Technologies for Electric Vehicles, DOE/ID-10243, 1989.

[4] D.B. Edwards, B. Carter, A high power, sealed, lead–acid battery for electric vehicles, J. Eng. Ind. 112 (1990) 293–298.

[5] J. Alzieu, J. Robert, J. Power Sources 13 (1984) 93–100.

[6] J. Alzieu, N. Koechlin, J. Robert, J. Electrochem. Soc., (1987) 1881–1884.

[7] K. Takahashi, M. Tsubota, K. Yonezu, K. Ando, J. Electrochem. Soc. 130 (1983) 2144–2149.

[8] J. Landfors, J. Power Sources 30 (1990) 131–141.

[9] D.B. Edwards, R.L. Cantrell, T. Dayton, Predicting the Performance of Batteries Having Paste Additives, The Twelfth Annual Battery Conference, IEEE 97th 8226, California State University, Long Beach, CA, 1997.

[10] D.B. Edwardsm, P.W. Appel, Conductivity model for lead–acid battery electrodes discharged at low rates, J. Power Sources 38 (1992) 218–286.

[11] P.W. Appel, D.B. Edwards, T. Stalick, Modeling the effects of electrolyte diffusion and paste conductivity on lead–acid battery performance, J. Power Sources 46 (1993) 49–60.

[12] D.B. Edwards, P.W. Appel, Modeling lead–acid batteries that have positive electrodes containing hollow, glass microspheres, J. Power Sources 46 (1993) 39–48.

[13] R.L. Cantrell, D.B. Edwards, P.S. Gill, Predicting lead–acid battery electrode performance using finite difference equations, J. Power Sources 73 (1998) 204–215.

[14] P.W. Appel, D.B. Edwards, Understanding and defeating the physical mechanisms limiting the capacity of lead–acid batteries, Adv. Perform. Mater. 3 (1996) 43–45.

[15] H. Metzendor, The capacity limiting role of the electronic conductivity of the active material in lead–acid batteries during discharge, J. Power Sources 7 (1982) 281–291.

[16] J.P. Pohl, W. Schendler, The electronic conductivity of compact lead dioxide samples with various stoichiometric compositions, J. Power Sources 6 (1981) 245–250.

[17] D.B. Edwards, An Electric Vehicle Design Based on a High-Power, Sealed, Lead–Acid Battery, SAE Technical Paper Series, 881790, 1988.